The International Journal of Advanced Manufacturing Technology (2023) 126:2147–2157
https://doi.org/10.1007/s00170-023-11243-1

ORIGINAL ARTICLE

Influence of a prolonged shelf time on PA12 laser sintering powder and resulting part properties

Sven Helge Klippstein[1] · Ivo Kletetzka[1] · Ilknur Sural[1] · Hans-Joachim Schmid[1]

Received: 22 November 2022 / Accepted: 8 March 2023 / Published online: 18 March 2023

Abstract
In the laser sintering technology, the semi-crystalline polymer material is exposed to elevated temperatures during processing, which leads to serious material ageing for most materials. This has already been investigated intensively by various authors. However, the ageing of the material at ambient temperatures during shelf life has not been the focus so far. The need to analyse the shelf life can be derived from an ecological and economic point of view. This work is focusing on the shelf life of *PA2200* (PA12). To reduce the potential influences of powder production fluctuations, two different powder batches stored for 5.5 years and 6.5 years are investigated and compared to a reference powder produced 0.5 years before these investigations. Multiple powder analyses and part characterisations have been performed. A significant yellowing and molecular chain length reduction can be derived from the measurement results. Whereas the influence on mechanical part performance was minor, the parts built with the stored powders are more yellowish. As it is most likely that this is due to the consumption of polyamide stabilisers, it can be assumed that these parts will be subject to significantly faster ageing. Therefore, it is still not recommended to use the stored powders for critical parts or light intense and humid environments.

Keywords Selective laser sintering · Shelf life · Polyamide 12 powder · *PA2200* · Material ageing

1 Introduction

In previous studies on laser sintering, the focus was mainly on powder ageing during the build process and cool-down times. Various investigations have already been carried out in this area to gain a better understanding of the process [1–9]. The ageing of new powder due to storage under normal, ambient conditions, on the other hand, has not yet been adequately analysed. Since laser sintering powder is very expensive and at the same time its quality is critical for the process, the aim to reduce the disposal of powder is of great interest from an ecological as well as an economical point of view. In this study, the shelf-life ageing effects of *PA2200* purchased from *EOS GmbH* are investigated [10].

In general, the ageing of a material is defined as the totality of all chemical and physical processes irreversibly occurring in a material over time [11]. Since many influencing factors overlap at the same time, a clear assignment of the property changes to respective causes is often not possible. In general, the ageing mechanisms can be classified into different subgroups. It can be distinguished between internal and external caused ageing effects or chemical and physical related ageing effects (compare Fig. 1). Again, the effects of different ageing processes can overlap, and make it difficult to clearly correlate a change in material properties with just one ageing mechanism [12]. Since most ageing effects are temperature dependent, it can take years at room temperature for material or part properties to change significantly.

Chemical ageing mechanisms comprise changes in the chemical composition, molecular structure, and/or molecular size of the material [11]. Most prominent are hydrolysis, post-condensation, post-polymerisation, oxidation, and degradation reactions. These processes are irreversible [13–16].

Physical ageing mechanisms are processes with changes in the microstructure, the molecular order, and the concentration ratio of the components (for multicomponent systems), e.g. absorption or loss of volatile components, respectively. Furthermore, changes in the external shape and structure or of measurable physical properties belong to physical material

✉ Sven Helge Klippstein
Helge.Klippstein@dmrc.de

Hans-Joachim Schmid
hans-joachim.schmid@upb.de

[1] Direct Manufacturing Research Center, Paderborn University, Paderborn, Germany

ageing, provided that the chemical ageing processes are not the cause [11]. The most important processes are relaxation/retardation, post-crystallisation, loss/migration of plasticizers, segregation, and agglomeration. Those processes can be reversible, which often requires remelting of the polymer [13–16].

The powders investigated here were stored in a typical storage room, most of the time in the basement room of the building. For the storing conditions, the following assumptions can be made:

- The storage temperature has never exceeded the glass transition temperature of ~ 50 °C [17];
- The relative humidity was in the range of 20–50%;
- The powder was stored in its original EOS packing (lightproof cardboard boxes with open plastic bags that are not airtight).

We suppose that the most important ageing mechanisms during shelf storage are the following:

(Thermo-)oxidative ageing A prerequisite for oxidative degradation is the presence of oxygen; thermal stress accelerates the degradation, which can be described by the Arrhenius equation [14]. Still, the PA12 is subject to oxidative ageing even under normal storage conditions, thus lower than the glass transition temperature of the material [18]. It should be noted that polymer powder has a significantly higher surface area compared to granulate or final components and is therefore more sensitive to ageing processes that depend on adsorption and diffusion processes. The oxidative degradation is triggered by radicals. In general, a radical is a molecule with a free electron, which leads to the separation of polymer components by further reactions with polymer chains, causing the formation of new radicals [19]. The systematics of the chemical processes is shown in Table 1. The attack of oxygen (O_2) on the carbon-hydrogen bond (CH_2) of a polymer chain forms a peroxide. As the oxygen single bond of the peroxide is unstable, it splits. This results in the separation of the electron pair and the formation of two primary radicals with dangling bonds. In the next step, the primary radicals react with undamaged polymer chains. In this example, the H atom of the polymer chain passes to the radical, so that the radical function is now passed on to the polymer chain and H_2O is formed from the radical. Here, the formation of water is unfavourable for the polymer since it additionally favours hydrolysis [13]. The new radicals can recombine with the oxygen atoms that are eager to bond. This bonding creates a new peroxide radical, which reacts again with an H atom of an undamaged polymer chain, again creating new radicals. Therefore, it should be noted that with each oxidation, the amount of radicals increases, and thus the ageing process is accelerated over time [13, 19].

This process continues until a termination reaction is introduced or the increase in radical concentration leads to reactions between them, such as the formation of a new polymer chain by two previously damaged polymer chains. Reactions between radicals thus aim at the extension or branching of polymer chains. In addition to transfer reactions, radicals can also lead to rearrangements of polymer chains. In this process, the lengths of the polymer chains are shortened or even halved. Due to a large number of those processes, oxidative ageing leads to a broad molar mass distribution with a variety of structures of the polymer chains. Stabilisers are added to the polymer to retard the thermo-oxidative ageing of LS polyamide [20]. The stabilisers typically react with radicals to prevent accelerated chain degradation and are consumed in the process. The stabilisers typically used in polyamides turn yellow in the process and therefore cause yellowing of the part during ageing of the material [21].

It should be mentioned that in semi-crystalline polymers, the rate of radical formation and oxygen diffusion depends on the degree of crystallisation. The reason for this is that oxygen cannot penetrate crystalline areas due to their high density. Therefore, oxidation takes place only in amorphous regions [22].

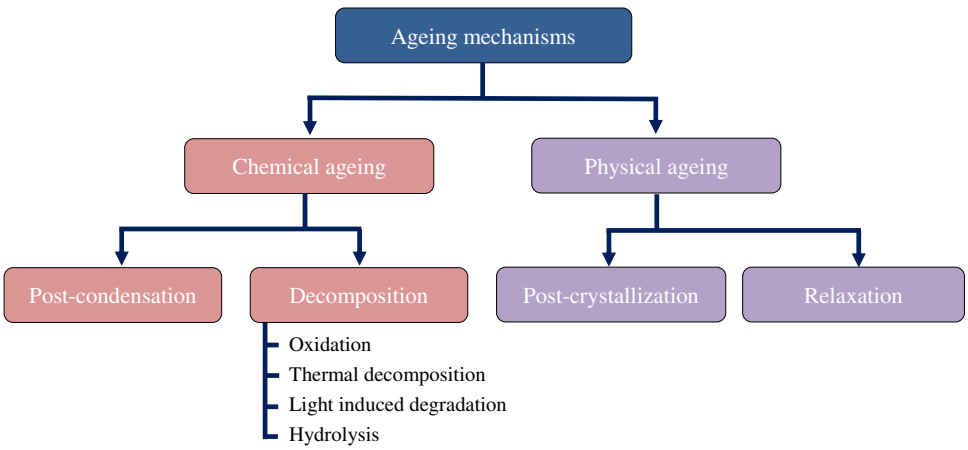

Fig. 1 Schematic of polymer ageing with the for storage most important decomposition mechanism [10]

Table 1 The four steps of oxidation on carbon-hydrogen bonds of polymers (simplified, based on [20]) and the schematic of hydrolysis-/polycondensation reactions

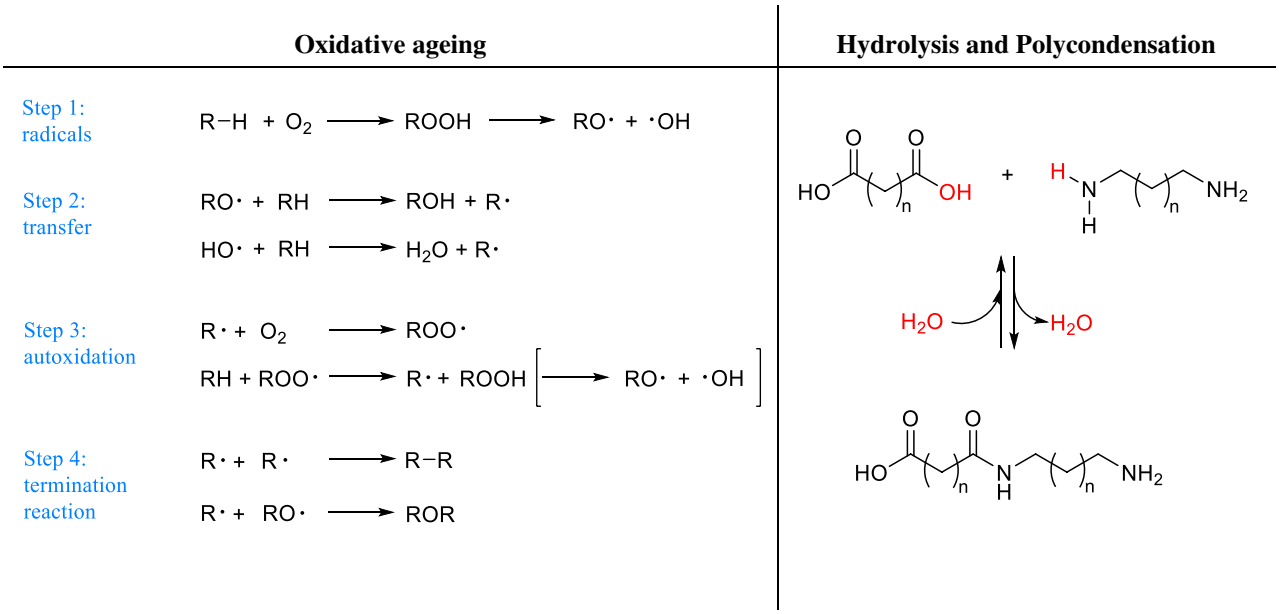

Hydrolysis is another form of chemical ageing. Due to atmospheric moisture and the formation of water molecules as a by-product of oxidative ageing, hydrolysis is also an ageing process, which can occur during storage. In general, hydrolysis can be explained as a reverse reaction of polycondensation, as polycondensation is an equilibrium reaction. The reaction mechanism is shown in Table 1 for the oxidative ageing and the related hydrolysis. Whereas in the polymerisation reaction two polymer chains are joined by splitting off water, hydrolysis leads to the scission of a polymer chain by reacting with H_2O [17].

Depending on the type, polyamides absorb different amounts of water [23]. Again, compared to granulation, powders can absorb water much faster due to the high surface area. As a result of hydrolysis reactions, the average molecular weight decreases and the range of molecular weight distribution increases. In addition, properties related to molecular weight, such as viscosity, are affected [20].

Thermal decomposition, light-induced degradation, and post-condensation are further chemical ageing processes, but due to the storing conditions, it is unlikely that these mechanisms take effect. Post-condensation can occur for polyamides because the chain ends of polyamides are still reactive after the synthesis reaction and can combine. Just like the polycondensation reaction during synthesis, post-condensation increases the average molecular weight. Post-condensation can take place in both the liquid and solid phases. However, this requires mobility of the reactive chain ends. Therefore, post-condensation typically takes place only above the glass transition temperature [12]. Since the storage temperature is well below the glass transition temperature, post-condensation is not considered further. Due to the same reason, thermal decomposition is not considered. Radiation or light-induced ageing is a decomposition reaction that is caused by radicals, just like oxidative ageing. Here, the free radicals are caused by electromagnetic waves (e.g. light). Since the powder was stored in cardboard boxes in a windowless storage room, light-induced ageing is also not relevant for the investigated powder.

Post-crystallisation as a physical ageing mechanism could theoretically impact the thermal processing window of the material by altering the melting temperature. However, post-crystallisation typically occurs above the glass transition temperature. If the powder was affected by post-crystallisation, this would be visible in differential scanning calorimetry (DSC) measurements [12].

2 Materials and methods

For the powder analytics, the virgin powder as well as the recycling powder from each batch were investigated. These powders do differentiate based on the years stored. As a reference, a freshly purchased powder was used. All investigations have been done in the period of 5 months starting in October 2021.

- Batch 918,216 (produced in March 2015) stored for ca. 6.5 years;

- Batch 918,422 (produced in July 2016) stored for ca. 5.5 years;
- Batch 919,336 (produced in August 2021) stored for less than 0.5 years (reference).

Additionally, all virgin powders were mixed with standard recycling powder (RP) out of the silo for building jobs on an *EOS P3* system. It can be assumed that this recycling powder is, on average, not older than 1 year, as it is taken from everyday laboratory work. An additional test was carried out with the oldest, 6.5-year-old powder. Here, used powder from batch 918,216 was generated by building a job with 100% virgin powder from this batch. Then, a 50/50 powder mixture of virgin and recycled powder from batch 918,216 was created and processed on an *EOS P3* system. The comparison of regular laboratory-used recycling powder and the stored recycling powder could indicate excessive ageing of stored powder during processing. For a simplified reading, the powders will be named based on the age at the time of this investigation.

Most polymers decolourise in a yellowing tone when the polymer chains degrade, e.g. due to ageing. For the measurement of the powder's yellowness values, a colourimeter *CR-410* from Konica Minolta was used. All measurements were repeated five times, following the CIELab system of the DIN EN ISO 11664–4, where the + b value is measured and analysed [24].

The particle size distribution (PSD) was measured by the dynamic image analyser *QICPIC* from Sympatec according to ISO 13322–2. The powder was dry dispersed by compressed air. The analyser takes up to 500 images per second of the particle projections, enabling the measurement of the number, a projected area equivalent to particle size, circularity, etc. The used measuring range (M5) allows the detection of particles with a size between 1.8 and 3755 µm. For each measurement, the amount of two heaped spatulas was used. The sample was taken from five different positions within the powder bags and mixed before testing [25].

The flowability of the powder was measured with a Mercury Scientific Inc. revolution powder analyser (RPA). The amount of 100 cm^3 powder was applied to the rotating aluminium drum with a borosilicate glass lid. The measurements have been taken at 3 min^{-1} rotational speed. For the measurement, 150 avalanches have been analysed, whereby each batch was measured three times but always with fresh powder to prevent measurement inaccuracies due to triboelectrically charged. After each measurement, the drum was cleaned and discharged with isopropanol. All measurements have been performed on the same day.

The melt volume flow rate (MVR) measurements were performed with a ZwickRoell Mflow based on DIN EN ISO 1133. For the measurement, a 4.0 g sample was dried at 105 °C for 20 min in an oven and directly afterwards applied to the machine. Here, a 300-s preheating at 235 °C with a test weight of 5 kg has took place before the nozzle was opened and the measurement started [26].

The differential scanning calorimetry (DSC) measurements were done with the DSC Polyma 214 from *NETZSCH*. The DSC measurements were performed based on the DIN EN ISO 11357. The heating and cooling ramps were set to ± 10 K/min; the starting temperature is 20 °C, then the sample is heated up to 250 °C and cooled down to the starting temperature again. This cycle was repeated twice to isolate the real material properties from the history, e.g. higher crystallinity due to tempering processes, etc. The full measurement was done under nitrogen protective gas. Each powder was tested three times to identify potential variations in the powders or measurements [27].

For determining the isothermal crystallisation time, the sample was melted and hold at 250 °C for 10 min and then quench-cooled down to 162 °C with 100 K/min, whereby the temperature was held for 2 h. The quench temperature was determined in multiple pre-measurements. At 162 °C, the recrystallisation peak could be identified as the cleanest. Each powder was tested three times with the same setting, as the measurement is very sensitive. Time position of the crystallisation peak was measured for each sample. Several pretests have been done to identify a representative isothermal temperature with starting conditions as stable as possible.

Measurements of the oxidation induction time (OIT) were carried out based on DIN EN ISO 11357–6. The sample is heated under nitrogen-protective gas up to 200 °C at a rate of 10 K/min. After holding the temperature for 5 min, the sample is exposed to a mixture of nitrogen and oxygen gas in a ratio of 50/50%. The oxidation induction time is measured from the start of the exposure to the onset of the decomposition reaction of the sample [28].

To test the part properties of these powders, the same test job was built for each powder batch. Therefore, the powder was mixed in a ratio of 50:50 with silo powder (recycling powder) or aged powder from the same batch, as explained previously. As presented in Fig. 2, the build job has two layers of tensile test specimens in a flat orientation. Additionally, a dimension measurement specimen and density cubes are included. All other parts are used to simulate a standard build job with standard packing density. All build jobs have been manufactured on an *EOS P395* system with 179 °C build temperature and the 120 µm part properties profile with *EOS* standard exposure settings.

All tensile bars of type 1A have been tested following the ISO DIN EN 527. For the measurements, an Instron Universal Testing System 5569 with a 5 kN load cell was used. The test velocity for determination of Young's modulus was set to 1 mm/min and switched after a strain of 0.3% to 50 mm/min for the rest of the test [29, 30].

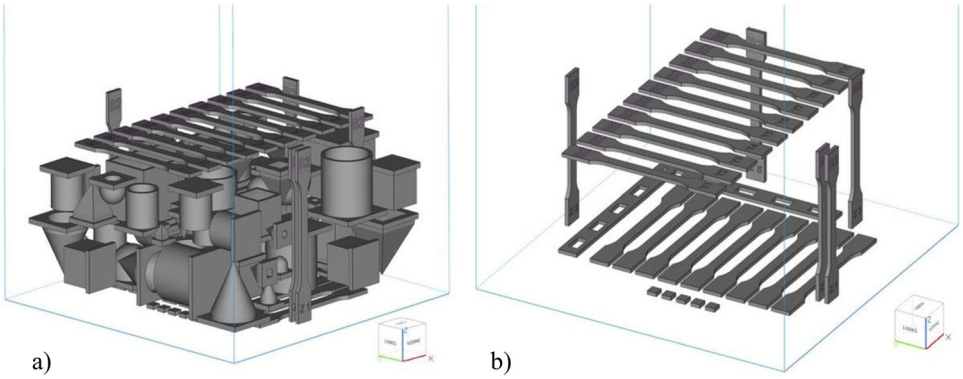

Fig. 2 Build job layout: **a** all specimens visible; **b** only tensile bars, density cubes and dimension specimens visible

To prevent water absorption, the dry-conditioned specimens have been stored with silica pads in closed bags after the build job and have been removed only immediately before testing. The wet-conditioned specimens have been treated based on the DIN ISO 1110 for 7 days at 70 °C and relative humidity (RH) of 62% [31].

The part surface is measured on a 90°-oriented surface, always of a part from, the same position within each build job. The 90° surface is orthogonal to each layer. For measurement, the fringe-light 3D-Profilometer VR 3100 from Keyence was used with a magnification factor of × 40. On the raw data, a Gaussian filter was applied to reduce irregular material reflections.

3 Results

First, the powder analysis results are presented, subsequently followed by the part properties measurements of the four test build jobs. A slight difference in the powder colour was visible already with the bare eyes (Fig. 3c). The discolouration was analysed based on the CIELAB colour space, whereby the yellowing index is b^*. A higher positive value for b^* is related to a stronger yellowing of the material. The measurements show a very low standard deviation for the five repetitions, as presented in Fig. 3, for the three powder batches as virgin and recycled powder. The yellow values of the recycled powders have increased significantly due to the thermal load (thermal ageing) during the build process. At the same time, an increasing yellowing of the virgin powders can be seen with increasing storage time; hence, there is a correlation between ageing and storage time. The yellowing is expected to be related to (thermo-) oxidative ageing. It is assumed that copper iodide is used as stabiliser and antioxidant. Copper halogen salts like copper iodide are often used for stabilising polyamides, as it shows superior stabilisation behaviour for polyamides at evaluated temperatures higher than 165 °C and act as UV stabiliser as well. Furthermore, yellowing is a known disadvantage of this stabiliser [13, 19].

The particle size distributions of the three powder batches show a homogeneous and narrow particle size distribution (Fig. 4), which is known to be advantageous for all powder bed fusion processes. However, a minor shift to larger particle sizes for the stored powders can be seen. Hence, it can be concluded that the stored powders have slightly larger particles than the reference powder, which can be explained either by production-specific fluctuations or agglomerate formation. Agglomerate formation is mainly depending on the

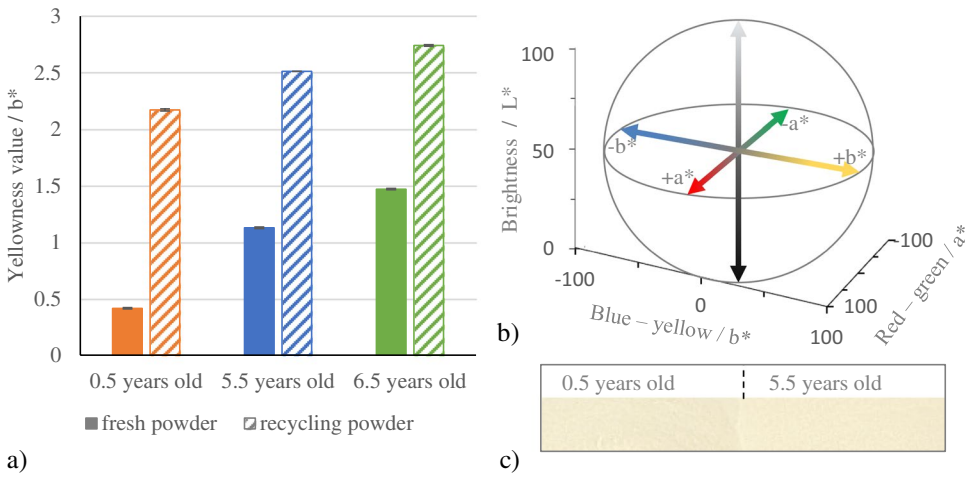

Fig. 3 **a** Yellowness measurements of the virgin and processed (i.e. recycled) powders; **b** CIELAB colour space; **c** image of 0.5-year-old powder and 5.5-year-old powder with visible colour differences in the yellow tone

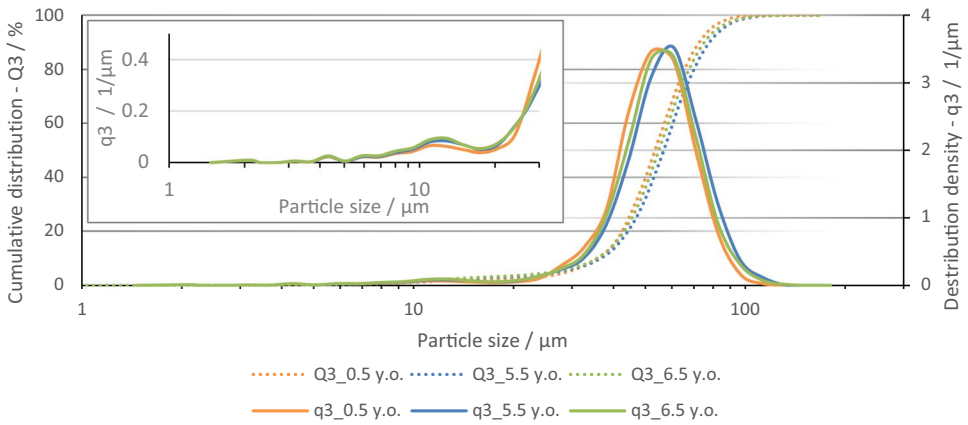

Fig. 4 Particle size distribution measured with dynamic image analysis (Sympatec QICPIC)

particle size, moisture, and electrostatic charging. In the case of very fine particles, the Van der Waals forces dominate the adhesive properties between the particles. In the case of moisture absorption, liquid bridges are responsible for the adhesion of the particles. A minimally increased fine content of the older powders can be seen in contrast to the reference powder (0.5 year old). But scanning electronic microscopy images (Fig. 5) have not shown any obvious differences between the powders and no signs of increased agglomeration for the stored powders. To determine the influences of the minimal changes in the PSD, the powder flowability is investigated with the revolution powder analyser.

For the revolution powder analyser measurements, the angle before an avalanche is measured, with the powder reaching the highest point of the drum beforehand. The smaller the angle, the better the flowability. At the same time, a narrow distribution is compulsory for good flowability. The curve of the 6.5-year-old virgin powder in Fig. 6 is further to the left. This means that the powder has smaller avalanche angles in total and thus flows better. Furthermore, a narrow distribution (33.04–48.33°) can be seen, which is also an indicator of a good flowing powder. The curves of 5.5-year-old powder are further to the right, with a narrow distribution (34.63–49.56°) similar to that of the 6.5-year-old powder. The curves of the reference powders (0.5 year old) show larger angles and an increased spreading, which indicates slightly poorer flowability.

The melt viscosity depends on the molecular weight and, therefore, also on the chain length. Short chain lengths and thus low molar masses lead to the high mobility of the macromolecules and consequently to low viscosity. Figure 7 shows the melt volume-flow rate values of the three virgin powder batches and the corresponding recycling powders. It can be seen that the values of the new powders differ from those of the recycled powders. Due to post-condensation in the build process, which is leading to molecular chain growth, the viscosity of the recycled powders is increased. In contrast, an increase in the MVR value with increasing storage time for the virgin powders is visible, hence the viscosity decreases. The same development can be seen in the MVR values of the recycled powders. The slope of the MVR values as a function of storage time is an indication that the changes are not due to batch fluctuations but are indicative of ageing.

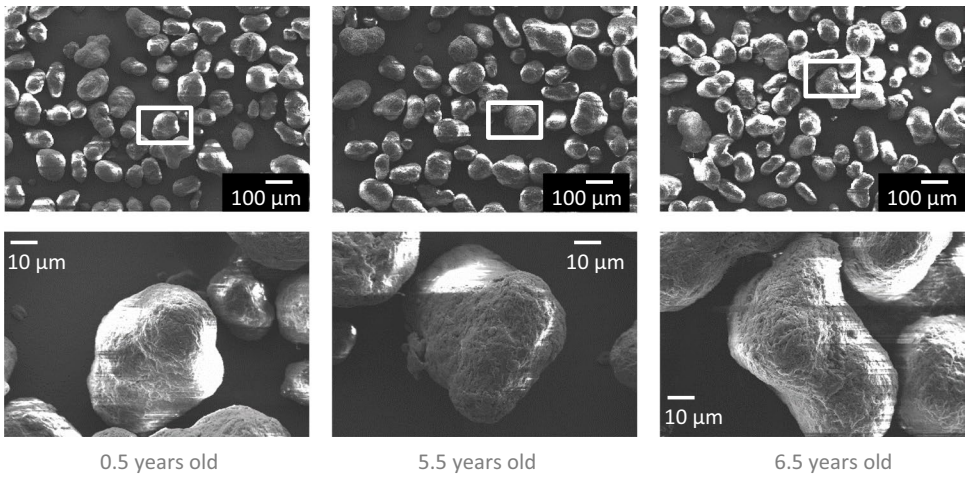

Fig. 5 Scanning electron microscopy images of the different powders

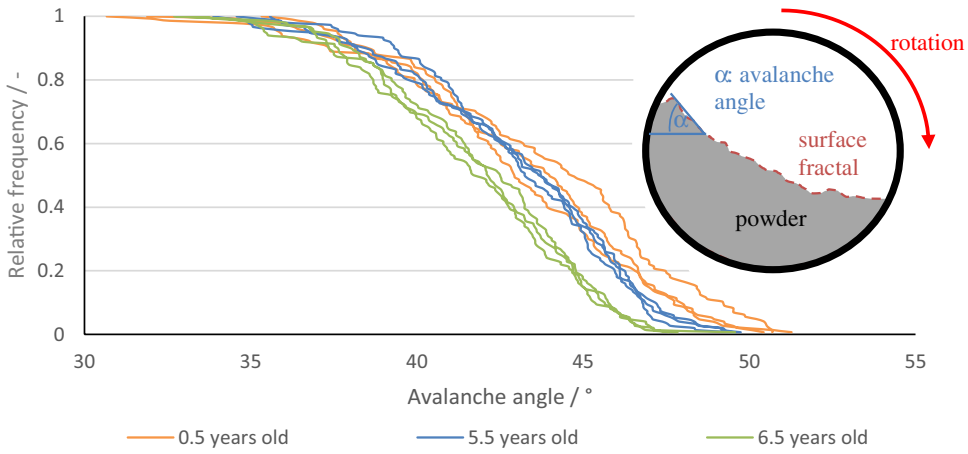

Fig. 6 Revolution powder analyser–relative frequency over avalanche angle for all three powders

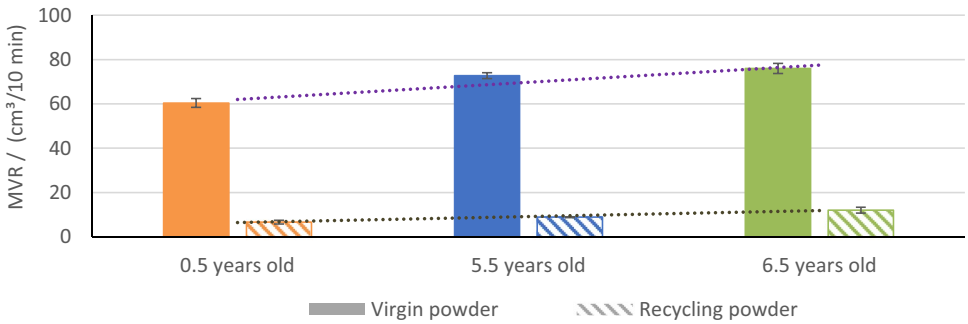

Fig. 7 Melt volume rate: 4 g sample weight measured at 235 °C and 5 kg load

It can be concluded that the molecular weight of the stored powders has decreased due to the storage period and the associated ageing mechanisms, such as oxidative ageing or hydrolysis.

The differential scanning calorimetry measurements are presented in Fig. 8, whereby the full line is representing the first cycle and the second cycle is represented by the dotted lines. It can be seen that the phase transition temperatures of the powder batches 5.5 and 6.5 years old are very similar. The sintering window of the two stored powders is significantly about 3 °C smaller compared (Fig. 8b) to the reference powder, mostly due to the earlier recrystallisation onsets. The same behaviour is observed for the second cycle, where the thermal histories of the samples have no influence on the measurements anymore.

One major influence on the crystallisation temperature is the nucleation agents. Powder additives like silica flow aid or fillers can act as nucleation agents. However, a change in the amount of additives in the powder is less likely, as this can only be the case if the manufacturing batch-to-batch fluctuation is very high or there has been a change in recipe within the powder production process. More likely is an effect related to the material's ageing. It has been observed that for polyamides, low molecular weight oligomers produced by chain scission can act as nucleating agents [32].

Typically, the specific enthalpy for melting in the first heating cycle is significantly higher for all powders compared to the second cycle. The melting enthalpy in the first cycle is almost identical for all three batches, indicating that no post crystallisation has occurred. Comparing the first cycle recrystallisation process, the stored powders required more specific enthalpy for solidification, which again can be due to higher crystallinity related to more nucleation seeds. A small shift of the exothermic crystallisation peaks between the first and the second cooling cycle is seen for all powders, which is typical and of no interest to the SLS process.

For the determination of the isothermal crystallisation temperature, the onset point should be used. With the combination of the Netzsch Polyma 214 and *PA2200*, this point could not be determined unquestionably, as after fast cooldown (100 K/min) to the isothermal recrystallisation temperature, there were no stable conditions found at any temperature levels. Thus, the peak temperature was used as measurement for the three powders (Fig. 9b). For analysis, three samples have been measured for each powder. The recrystallisation time is based on the average of each test and is shown in Fig. 9a. As the stored powders (5.5 and 6.5 years old) show again earlier recrystallisation at constant temperature, the nucleating agent hypothesis is supported. Analysing the oxidation induction time revealed significantly reduced

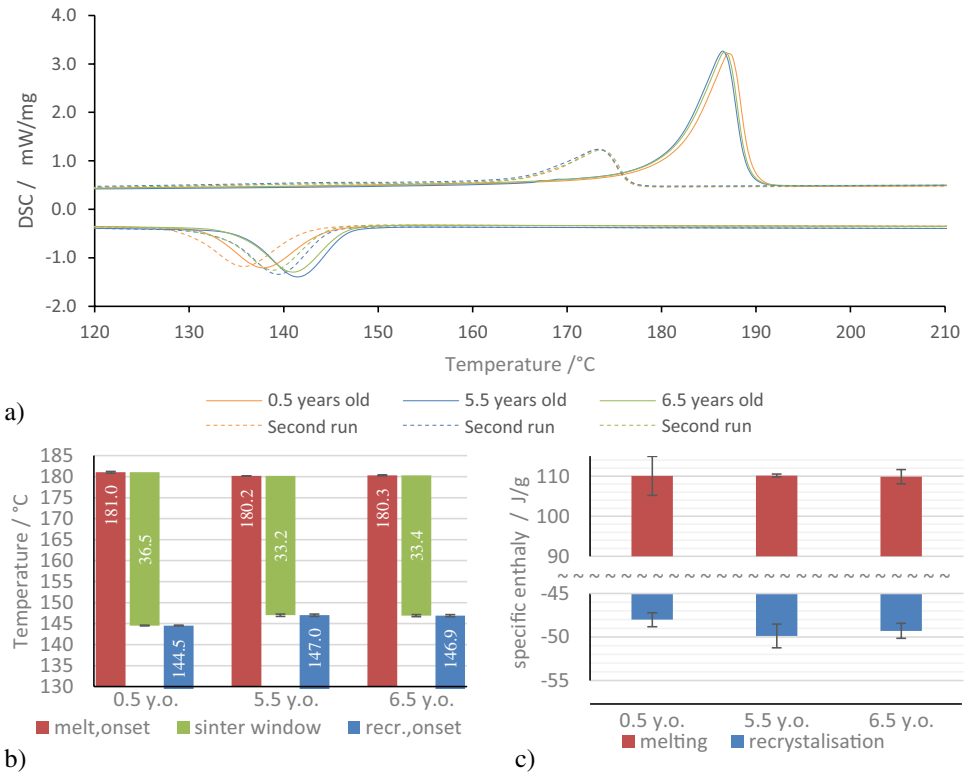

Fig. 8 DSC measurements of the virgin powders with three measurements per powder **a** exemplary DSC graph per powder; **b** sinter window analysis; **c** specific enthalpy analysis (first cycle)

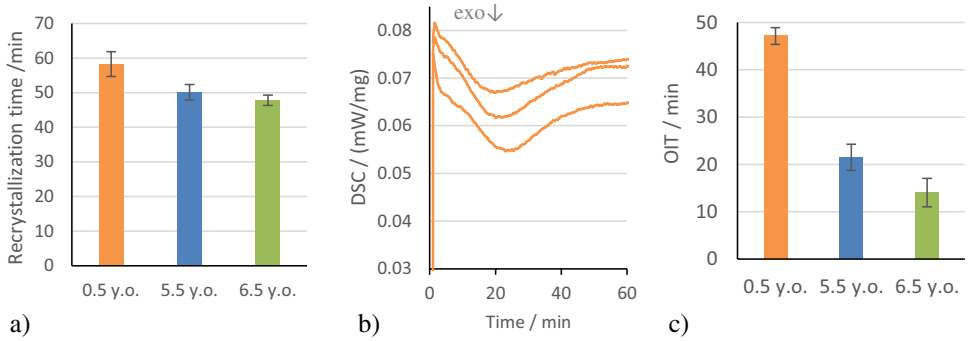

Fig. 9 Isothermal crystallisation temperature analysis: **a** recrystallisation at 162 °C; **b** the 3 DSC measurements for the reference virgin powder; **c** oxidation induction time analysis of all three powder batches (virgin)

values for the stored powders, as shown in Fig. 9c. This supports the thesis from the yellowing index measurement that the antioxidants are degraded over time and the material is less resistant to oxidative degradation after prolonged storage durations.

After mixing the powders, preparing the machine, and running the build jobs, the tensile properties can be analysed. The mechanical performance of the parts built with the same regular recycled powder from the *EOS* powder loop silo shows no significant changes; compare to Fig. 10. The tensile strength, elongation at break, and Young's modulus are significantly influenced by the conditioning procedure for 7 days at 70 °C and 62% RH. However, all three build jobs with regular recycling powder seem to perform in a fluctuation range within the standard deviation of the process itself [33]. For the fourth builfd job, 6.5-year-old powder that has already been processed once was used as recycling powder for creating the 50/50 mixed powder with virgin 6.5-year-old powder. For this test, the tensile properties showed a noticeable difference compared to the reference batch. The tensile strength was lower, especially after conditioning, and the parts exhibited a higher stiffness in the dry state.

Additionally, the long-term properties of parts built with the stored powder batches might fall off drastically as soon as all stabilisers are consumed and the oxidation processes are accelerated, damaging the polymer chains. Although long-time experiments were out of scope for these investigations, it can be expected that an embrittlement and premature failure of these parts in use will occur.

Furthermore, the surface roughness of planes printed in the *z* direction was analysed. Two effects might lead to

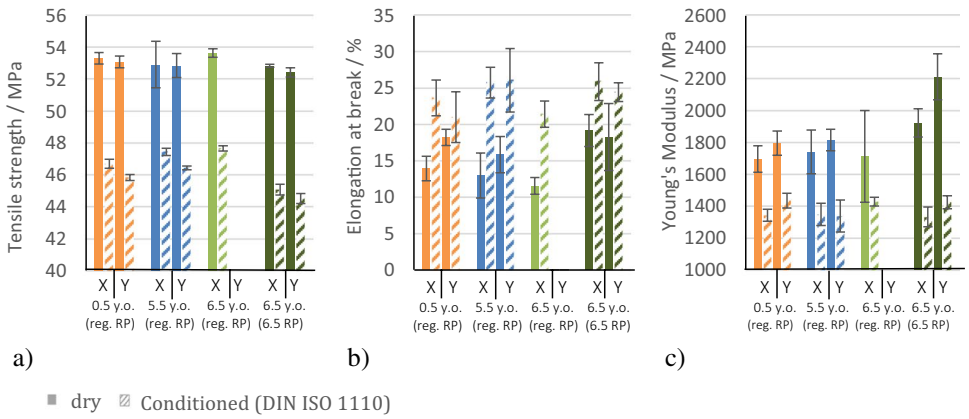

Fig. 10 Tensile test measurement results for dry and wet conditions: **a** tensile strength; **b** elongation at break; **c** Young's modulus

a change in the part's surface roughness. For the stored powders, the PSD is slightly larger, and it is known that the melt viscosity can influence the part surface and might even lead to surface defects. If the viscosity is too high, the parts show orange peel defects. If viscosity is too low, the part dimensions get worse, and more particles might get loosely attached to the part's surface. The stored powder exhibited a lower melt viscosity; however, the measurements (Fig. 11a) showed only minor differences for the powder batches. There was only a slight trend towards rougher surfaces with increased storage duration.

The part density can be taken as an indication of potential pores within the part. If the laser exposure parameter is kept constant, the melt viscosity still can influence the porosity of the parts. As the melt viscosity decreases, better coalescence is expected, leading to less pores. However, the part density is not influenced significantly. There are little variations between the two stored powders, but those are assumed to be standard build and measurement deviations (Fig. 11b). Especially as the build job with the 6.5-year-old powder does show the roughest surface, which often leads to small gas bubbles adhering to the part surface. If those bubbles are not removed completely, they do reduce the precision of the density measurement using the Archimedes method and result consequently in decreased density values.

To check the powder storage time influence on the part defect probability, microscopic cross-section analysis, or XCT analysis, would be an option. However, those tests have been out of scope for this project but would be beneficial for the evaluation of the melt coalescence.

4 Conclusion

The measurement of the yellowing index, melt viscosity, thermal behaviour, and especially oxidation induction time showed significant differences between the stored and reference powder. The part properties, in contrast, did not show significant deviations between the reference and the stored powders mixed with regular recycling powder. However, the use of recycling powder from the same 6.5-year-old batch mixed with virgin 6.5-year-old powder caused a small shift in tensile properties.

From these results, some guidelines can be derived. However, it has to be kept in mind that the production-based batch-to-batch variation for some powder properties is unknown. It is assumed that insignificant deviations in the measurements are due to production and test fluctuations and significant deviations are due to ageing. Furthermore, as the exact composition of the powder is not known, the discussion is based on some speculations.

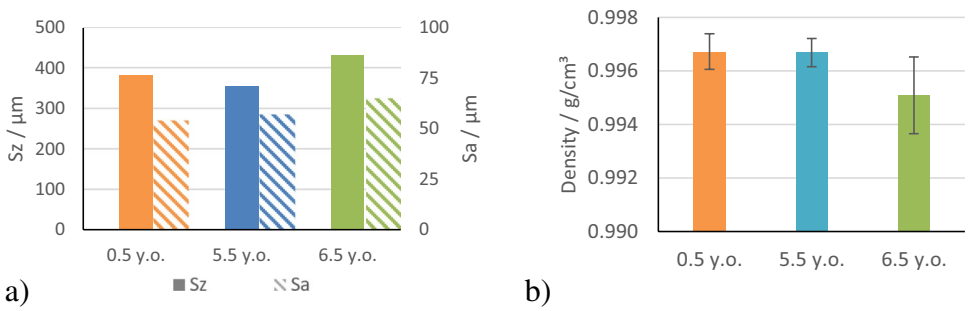

Fig. 11 **a** Fringed light surface measurements for 90° surface; **b** part density measurement by Archimedes' method

For example, the UV and oxidative stabiliser copper iodide is known to make a yellowish colour in polyamides, still, the *PA2200* is very white, as shown for the reference powder. The *PA2201* is a naturally coloured PA12 that is more transparent than the *PA2200*. Hence, it can be assumed that the here used *PA2200* is whitened with an additive. The measured yellowing of the stored powder can be caused by degradation of the copper iodide. Copper iodide is soluble in water, which is reported to lead to blume out of the parts resulting in discolouration. Following this theory, the virgin powders stored for 5.5 and 6.5 years show oxidative ageing effects. It is assumed that a significant share of the stabilisers has been degraded or washed out over the long shelf time even at low temperatures. This theory is supported by the significant reduction of the oxidative induction time for those materials.

Furthermore, water is a by-product of oxidative ageing, which in turn leads to hydrolysis in the material and consequently chain scission. Chain scission seems to be confirmed by the increased melt flow rate of these powders. As mentioned, oxidative ageing, hydrolysis, or a combination of both are expected to be the cause. An even better statement on the molecular chain length would be possible by the gel permeation chromatography (GPC) measurement. However, the MVR is pointing in the same direction and is considered to support this thesis sufficiently.

The revolution powder analyser measurements indicate that the flowability of the stored powders was only slightly higher. Furthermore, these powders showed a slightly larger particle size distribution. Whereby, only a view, even small agglomerates might lead to this shift in the particle size analysis. The SEM images have not shown any obvious changes in the particle shape or composition. But the detection of only small agglomerates is difficult with this small analysis area, as given by the SEM images. Nevertheless, variations from batch to batch cannot be ruled out.

The sintering window is decreased for the long-term stored powders as the recrystallisation temperature is higher. It is expected that nucleation agents are responsible for the earlier recrystallisation. There are two theories on those nucleation seeds: hydrolysis can lead to an increased concentration of oligomers, which can act as nucleation agents in the same way as an increased concentration of silica flow aids. Independent of the cause, the recrystallisation temperature is increased; therefore, the build temperature control has to be more precise in order to prevent curling. Still the process runs stable for most build job layouts and parts on an EOS P3 system.

All powder mixes could be built with the same settings, and the parts of those build jobs showed similar static mechanical properties. When the stored powder was not only used as a virgin powder for the 50:50 ratio of mixed powder but also for the recycled powder, the tensile strength was slightly decreased after conditioning and the parts exhibited a higher Young's modulus. The density was not impacted by the powder batch, while the surface roughness tended to increase slightly for the stored powder batches. As expected, the parts from the 5.5- and 6.5-year-old powder mixes are more yellow than the reference parts.

The long-term properties, like weathering, fatigue, or creep test, have not been measured for those parts yet. As the oxidative induction time for the stored powders showed a significant reduction, it can be assumed that the parts will age faster than the reference components during usage. Increased yellowing followed by embrittlement might be a consequence. Therefore, it is recommended to take the service environment into account for parts built from long-stored powders. Furthermore, critical parts should not be built with those powders, and the stored powders should be excluded from the closed-loop powder recycling system. Finally, it can be recommended that if LS powder has to be stored for a long period of time, an as inert as possible atmosphere should be used. The minimum recommendation would be a sealed bag in a dark location at low temperatures (suggestion: $T < 25$ °C) and low humidity (suggestion: RH < 30%).

Acknowledgements We would like to thank all DMRC industry partners for their sharing of knowledge.

Author contribution All authors contribute to the work, from conception to implementation and interpretation of the data. Most measurements have been done by Ilknur Sural, supported by Ivo Kletetzka and Helge Klippstein. Data analysis was done by all authors. The first draft of the manuscript was written by Helge Klippstein and Ivo Kletetzka, and all authors commented on previous versions of the manuscript. All authors read and approved the final manuscript.

Funding Open Access funding enabled and organized by Projekt DEAL.

Declarations

Conflict of interest The authors declare no competinginterests.

References

1. Josupeit S (2019) On the influence of thermal histories within part cakes on the polymer laser sintering process. Dissertation, Paderborn University
2. Josupeit S, Ordia L, Schmid H-J (2016) Modelling of temperatures and heat flow within laser sintered part cakes. Addit Manuf 189–196. https://doi.org/10.1016/j.addma.2016.06.002
3. Josupeit S, Schmid H-J (2016) Temperature history within laser sintered part cakes and its influence on process quality. Rapid Prototyp J 788–793. https://doi.org/10.1108/RPJ-11-2015-0166
4. Josupeit S, Schmid H-J, Tutzschky S et al (2015) Powder ageing and material properties of laser sintered polyamide 12 using low refresh rates. Proc Rapid Tech 63–78. https://doi.org/10.1007/978-3-662-48473-9_5
5. Kummert C, Diekmann W, Tews K et al. Influence of part microstructure on mechanical properties of PA6X laser sintered specimens. In: Proceedings of the 30nd Annual International Solid Freeform Fabrication Symposium, pp 735–744. https://utw10945.utweb.utexas.edu/2019-table-contents. Accessed 10 Nov 2022
6. Drummer D, Wudy K, Drexler M (n.d.) Modelling of the aging behavior of polyamide 12 powder during laser melting process 1664:1–5. https://doi.org/10.1063/1.4918514
7. Wudy K, Drummer D, Kühnlein F et al (n.d.) Influence of degradation behavior of polyamide 12 powders in laser sintering process on produced parts. 691–695. https://doi.org/10.1063/1.4873873
8. Dotchev K, Yusoff W (2009) Recycling of polyamide 12 based powders in the laser sintering process. Rapid Prototyp J 15:192–203. https://doi.org/10.1108/13552540910960299
9. Blattmeier M (2012) Strukturanalyse von lasergesinterten Schichtverbunden mit werkstoffmechanischen Methoden. Dissertation, Universität Duisburg-Essen. https://doi.org/10.1007/978-3-8348-2501-8
10. Kletetzka I, Klippstein SH, Sural I et al (2022) Shelf life of polyamide 12 (PA2200) laser sintering powder. In: Proceedings of the 33nd Annual International Solid Freeform Fabrication Symposium. https://utw10945.utweb.utexas.edu/2022-table-contents. Accessed 10 Nov 2022
11. DIN 50035:2012–09: Terms and definitions used on ageing of materials – polymeric materials
12. Baur E, Brinkmann S, Osswald T A, Schmachtenberg E (2013) Saechtling Kunststoff Taschenbuch, Hanser, München
13. Ehrenstein GW, Pongratz S (2013) Resistance and stability of polymers. Hanser, Munich
14. Ehrenstein GW (2001) Polymeric materials: structure - properties - applications. Hanser, Munich
15. Verdu J (2012) Oxidative ageing of polymers. Wiley, ISBN, p 9781848213364
16. White JR (2006) Polymer ageing: physics, chemistry or engineering? Time to reflect. C R Chim 9:1396–1408. https://doi.org/10.1016/j.crci.2006.07.008
17. Domininghaus H, Elsner P, Eyerer P et al (2012) Kunststoffe. Springer, Berlin Heidelberg, Berlin, Heidelberg
18. Kaiser W (2021) Kunststoffchemie für Ingenieure: Von der Synthese bis zur Anwendung, Hanser, München
19. Zweifel H (1998) Stabilization of polymeric materials. Springer, Berlin Heidelberg
20. Dahlmann R, Haberstroh E, Menges G (2022) Menges Werkstoffkunde Kunststoffe, Hanser, München
21. Maier R-D, Schiller M (2016) Handbuch Kunststoff-Additive, Hanser, München
22. Ehrenstein G (2011) Polymer-Werkstoffe: Struktur - Eigenschaften - Anwendung, Hanser, München
23. Hellerich W, Harsch G, Haenle S (2010) Werkstoff-Führer Kunststoffe: Eigenschaften, Prüfungen, Kennwerte, 10. Aufl. Carl Hanser Fachbuchverlag
24. DIN EN ISO/CIE 11664-4:2020-03 Farbmetrik - Teil 4: CIE 1976 L*a*b* Farbraum
25. ISO 13322-2:2021-12Partikelgrößenanalyse - Bildanalyseverfahren - Teil 2: Dynamische Bildanalyseverfahren
26. DIN EN ISO 1133-1:2022-10Kunststoffe - Bestimmung der Schmelze-Massefließrate (MFR) und der Schmelze-Volumenfließrate (MVR) von Thermoplasten
27. DIN EN ISO 11357-3:2018-07Kunststoffe - Dynamische Differenz-Thermoanalyse (DSC) - Teil 3: Bestimmung der Schmelz- und Kristallisationstemperatur und der Schmelz- und Kristallisationsenthalpie
28. DIN EN ISO 11357-6:2018-07Kunststoffe - Dynamische Differenz-Thermoanalyse (DSC) - Teil 6: Bestimmung der Oxidations-Induktionszeit (isothermische OIT) und Oxidations-Induktionstemperatur
29. DIN EN ISO 527-1:2019-12Kunststoffe - Bestimmung der Zugeigenschaften
30. DIN EN ISO 16396-2:2022-10Kunststoffe - Polyamid (PA)-Formmassen für das Spritzgießen und die Extrusion - Teil 2: Herstellung von Probekörpern und Bestimmung von Eigenschaften
31. DIN EN ISO 1110:2019-09Kunststoffe - Polyamide - Beschleunigte Konditionierung von Probekörpern
32. Zweifel H, Maier R-D, Schiller M et al (eds) (2009) Plastics additives handbook, 6th edn. Hanser, München
33. Klippstein H, Schmid H-J (2019) Methodik zur Qualifizierung des Lasersinter Prozesses für die Serienfertigung. In: Kynast M, Eichmann M, Witt G (eds) Rapid.Tech + FabCon 3.D International Hub for Additive Manufacturing, Hanser, München, pp 349–365